

# Compositional analysis of XVIII century glazed, polychrome, layered porcelain by non-destructive micro $\alpha$ -PIXE

A. Zucchiatti<sup>a,b</sup>, C. Pascual<sup>c</sup>, M.D. Ynsa<sup>a,\*</sup>, L. Castelli<sup>a</sup>, P. Recio<sup>c</sup>,  
E. Criado<sup>c</sup>, F.J. Valle<sup>c</sup>, A. Climent-Font<sup>a</sup>

<sup>a</sup> Centro de Micro Analisis de Materiales, Universidad Autonoma de Madrid, Carretera de Colmenar km 15, 28049 Madrid, Spain

<sup>b</sup> INFN, via Dodecaneso 33, 16146 Genova, Italy

<sup>c</sup> Instituto de Cerámica y Vidrio, CSIC. Kelsen, 5. Campus de Cantoblanco, 28049 Madrid, Spain

Received 25 May 2007; received in revised form 27 August 2007; accepted 1 September 2007

Available online 7 November 2007

## Abstract

A XVIII century polychrome porcelain, of complex layered structure has been analysed by using several techniques. The studied porcelain shard was a fragment of a flooring tile from the “Casita del Labrador”, a small palace located in Aranjuez, near Madrid. The high spatial resolution of the  $\alpha$ -PIXE technique, an appropriate choice of the beam energies and the use of an external micro-beam have allowed to determine the composition of the constituent layers almost free from interferences, which was not possible with other analytical techniques. The nature of the pigments in particular is now well understood. PIXE analysis was confirmed by traditional, although destructive, XRD, XRF and SEM-EDS analyses.  
© 2007 Elsevier Ltd. All rights reserved.

**Keywords:**  $\alpha$ -PIXE; Micro-beam; Painted layers; Porcelain; Glaze; Enamel; Buen Retiro

## 1. Introduction

Porcelain flooring tiles were some of the last known productions of Buen Retiro Factory (1759–1808). Buen Retiro was founded by Carlos III by reallocating artists, masters and workers, and even transporting raw materials and pastes from the primitive (1743–1759) Capodimonte (Naples) factory. Besides its artistic enterprise, in the second half of XVIII century, the main effort in Buen Retiro was to achieve the formula and to find the raw materials to manufacture the hard paste, or true porcelain. After many attempts, Bartolomé Sureda produced a new kind of hard paste by using quartz, feldspar and sepiolite, a magnesium clay, instead of kaolin. Porcelain tiling, which is still in place in two floors of the “Casita del Labrador” in Aranjuez, was an expensive and rare application of the hard paste; maybe with the aim of demonstrating the mechanical strength of this new hard porcelain formula.

## 2. The ceramic analyses of the porcelain

The sample, an approximately 140 mm  $\times$  70 mm fragment of a 140 mm  $\times$  140 mm tile, Fig. 1, was cut in small pieces to perform, beside the  $\alpha$ -particle induced X-ray emission (PIXE) study, X-ray diffraction (XRD), scanning electron microscopy-energy dispersive spectroscopy (SEM-EDS) and X-ray fluorescence (XRF) ceramic characterization. The sample, which was removed during a past restoration, is one of the elements of a flooring tiles collection conserved by *Patrimonio Nacional* in Aranjuez. Some of these pieces have been previously characterized by ceramic methods<sup>1</sup> to determine their composition and the mineralogical constituents of the body, the glaze and the decoration colours of the porcelain. In this work a new and representative tile of the series has been chosen in order to establish the capacity and the complementarity of the non-destructive micro  $\alpha$ -PIXE analysis versus analytical techniques well proved in ceramic research.

### 2.1. XRD, XRF and SEM-EDS analyses

XRD was carried out in a Siemens D5000 automated diffractometer using Cu K $\alpha$  radiation (1.5418 Å) and a sec-

\* Corresponding author. Tel.: +34 914973632; fax: +34 914973621.  
E-mail address: [m.ynsa@uam.es](mailto:m.ynsa@uam.es) (M.D. Ynsa).

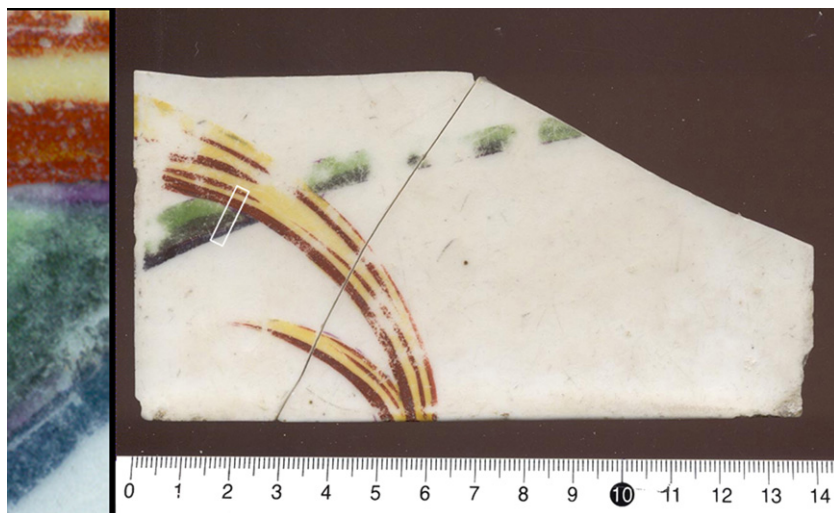


Fig. 1. The porcelain tile from the “Casita del Labrador”. On the left, the coloured area where the  $\alpha$ -PIXE beam was focussed.

ondary curved graphite monochromator. Crystalline  $\alpha$ -quartz,  $\alpha$ -cristobalite and protoenstatite, were identified in the porcelain body proving that the sample corresponds to the Sureda production.<sup>2</sup> Scanning electron microscopy in field emission, Hitachi S-4700 (FE-SEM), of a polished transversal cut of the sample displayed in Fig. 2 the three layers: porcelain body, glaze and enamel of the tiles. Fig. 3 shows the crystalline,  $\alpha$ -quartz,  $\alpha$ -cristobalite and protoenstatite, and the glassy phases forming the porcelain microstructure.

Chemical composition in the massive components, glaze and porcelain base, of the tile was accurately determined by X-ray fluorescence (XRF) in a Philips, MagiX SuperQ, fluorescence spectrometer with a 2.4 kW Rh X-ray generator.

## 2.2. The $\alpha$ -PIXE analysis of layered structures

Analytical techniques that make use of an ion beam can be exploited quite efficiently in the characterization of complex layered structures, as is the sample from Buen Retiro, since the

possibility of choosing an appropriate ion and the total control that we have on the particle energy and on the beam current allow us to quantify major, and minor elements in each of the expected layers and in a totally non-destructive way. In this case we know from scanning electron microscopy in field emission mode, Fig. 2, that over a body of porcelain lays a 110–120  $\mu\text{m}$  thick layer of potassic glaze. The ceramics decoration is applied in the form of pigmented lead enamel over the potassic glaze and has a variable thickness depending on the strength and speed of the brush strokes and on the will of the artist to reach a particular colour shade. In any case, from what is observed by SEM in the rest of the series, we expect for the painted layers a thickness not exceeding 20  $\mu\text{m}$ . The ranges of alpha particles and protons in both a lead and an alkaline glass have been calculated as a function of energy. In Fig. 4 it is clearly seen that to explore with protons a depth as small as 12  $\mu\text{m}$  would require an energy beam of 900 keV only and that the proton range will exceed 50  $\mu\text{m}$  with an energy above 2250 keV.

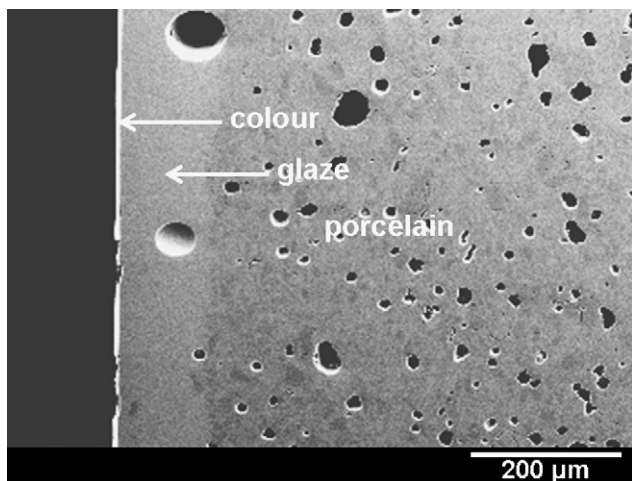


Fig. 2. Multilayer structure in a polished transversal cut of the tile.

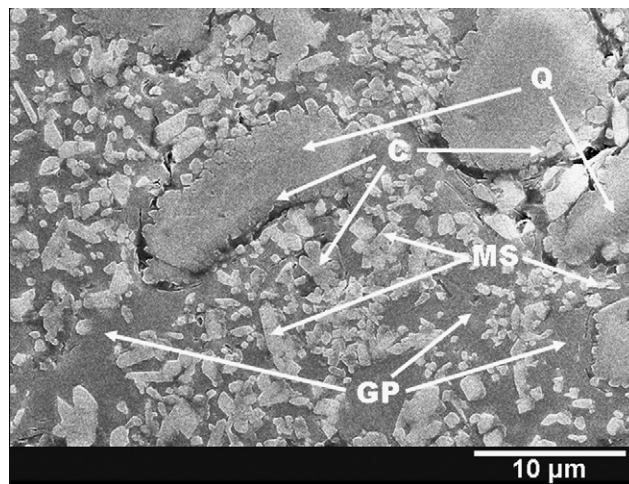


Fig. 3. Quartz (Q), cristobalite (C), protoenstatite (MS) and (GP) glassy phase in the porcelain.

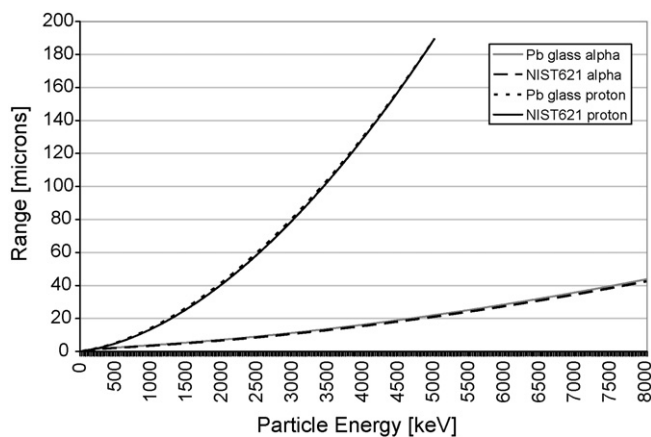


Fig. 4. The range of alphas and protons inside two representative materials: a lead glass and an alkaline glass standard (NIST621).

With alpha particles the derivative of the range versus energy curve is much smaller, which means that we can adjust the penetration depth with greater accuracy than with protons. Indeed alpha particles of 2500 keV will have a range of 8.85  $\mu\text{m}$  and will therefore be suitable for exploring from the surface the pigmented lead glass layer without interfering with the underlying glaze. Alpha particles of 8000 keV will have a range of about 42  $\mu\text{m}$ , i.e. they will be suitable for exploring the glaze from the surface without interfering in principle with the porcelain body. We have performed measurements at the micro-beam line<sup>3</sup> of the 5 MV Tandatron accelerator at the CMAM (Centro de Micro-Análisis de Materiales) in Madrid.<sup>4</sup> Alpha energies of 2500 and 8000 keV were selected as explained above. The uncertainty in the bombarding energy is better than  $\pm 0.1\%$ . The alpha beam crossed the 200 nm  $\text{Si}_3\text{N}_4$  exit window and 5 mm of He before reaching the target to minimize lateral straggling. It has been possible to use beams with about 100  $\mu\text{m}$  full width half maximum (FWHM). The width of the area analysed on each point of the sample is large enough to take an average composition of the porcelain (see Fig. 3), but also is narrow enough to discriminate quite well the different strokes on the colours of the enamel.

The X-rays are collected, quite traditionally by a 10 mm<sup>2</sup> Si(Li) detector with helium flow in front and by an 80 mm<sup>2</sup> Si(Li) detector with a 350  $\mu\text{m}$  mylar filter in front. This second detector sees characteristic X-rays from potassium to lead and has a peak of sensitivity for iron. The energy loss of 2500 keV alphas in the window and the helium gas is 290 keV, which means an impact energy of 2310 keV, while at 8000 keV is 130 keV, which means an impact energy of 7870 keV.

X-ray spectra have been analysed with the code GUPIX.<sup>5</sup> The product of detector solid angle and efficiency has been calculated for both detectors by adjusting the theoretical elemental yields given by the GUPIX package to measured yields in a series of standards of alkaline and lead glass so to reproduce within a few percent the certified concentrations. Once established the procedure was followed identically to determine the elemental concentrations in the porcelain sample: the concentration was taken from the detector in which each element was seen with better statistics or from the average of the two values when the statistics was similar.

### 3. Discussion of results

The compositions of the porcelain body and of the glaze are well established by the PIXE analysis and confirm SEM-EDS and XRF analyses.

Table 1 reflects the excellent accuracy in chemical composition of the porcelain determined by XRF, done on a powdered sample, and by surface non-destructive  $\alpha$ -PIXE analyses. Beside the MgO content, it must be noticed the low alkaline concentration and the total absence of PbO. All these characteristics are the fingerprint of Sureda porcelain.

The composition of the porcelain body corresponds to a paste formulated with quartz, feldspar and sepiolite. This last mineral, with chemical formula  $\text{Mg}_8\text{Si}_{12}\text{O}_{30}(\text{OH})_4(\text{H}_2\text{O})_4 \cdot 8\text{H}_2\text{O}$ , is a fibrous clay extracted from a quarry in the Vallecas area, near Madrid. It is responsible for the high Mg content in the material. In the fired porcelain, MgO is present both as protoenstatite, the high temperature form of  $\text{MgSiO}_3$ , and as a vitreous phase constituent.

Glaze is applied on the porcelain surface to get a dense and smooth layer where decoration is applied over. The XRF and the  $\alpha$ -PIXE analyses, outlined in Table 2, show the elemental composition of the glaze. XRF data were collected on a 27 mm diameter area on the white surface of the sample. As before  $\alpha$ -PIXE concentrations fit well with the corresponding XRF data in the glaze.

Table 1  
Chemical composition of porcelain body (in wt.%)

	$\alpha$ -PIXE (8.0 MeV)	$\alpha$ -PIXE (2.5 MeV)	XRF
$\text{Na}_2\text{O}$	0.55	0.90	0.49
$\text{MgO}$	13.34	12.39	12.42
$\text{Al}_2\text{O}_3$	3.51	3.85	4.65
$\text{SiO}_2$	79.23	79.81	79.81
$\text{K}_2\text{O}$	2.59	2.32	2.08
$\text{CaO}$	0.33	0.46	0.19
$\text{Fe}_2\text{O}_3$	0.33	0.28	0.36
$\text{Sb}_2\text{O}_5$	0.11	n.d.	n.d.
$\text{PbO}$	n.d.	n.d.	n.d.

Table 2  
Chemical composition of the glaze (in wt.%)

	$\alpha$ -PIXE (8.0 MeV)	$\alpha$ -PIXE (2.5 MeV)	XRF
$\text{Na}_2\text{O}$	3.23	3.44	2.8
$\text{MgO}$	1.24	0.75	0.79
$\text{Al}_2\text{O}_3$	16.49	18.50	18.8
$\text{SiO}_2$	66.70	64.44	66.7
$\text{P}_2\text{O}_5$	n.d.	n.d.	0.4
$\text{SO}_3$	n.d.	n.d.	0.1
$\text{K}_2\text{O}$	10.29	8.67	8.98
$\text{CaO}$	0.91	0.95	1.2
$\text{MnO}$	0.01	n.d.	n.d.
$\text{TiO}_2$	n.d.	n.d.	0.02
$\text{Fe}_2\text{O}_3$	0.11	0.11	0.14
$\text{CuO}$	0.01	n.d.	n.d.
$\text{SnO}_2$	0.50	n.d.	n.d.
$\text{PbO}$	0.27	1.85	0.011

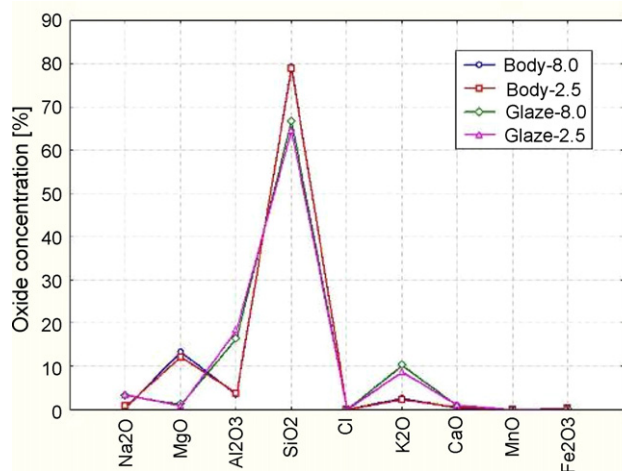


Fig. 5. The compositional profile of porcelain body and glaze given by  $\alpha$ -PIXE at two alpha energies.

The average of the glaze and the porcelain body profiles obtained at 2.5 and at 8.0 MeV are shown in Fig. 5. The compositions relative to the body are very close at 2500 and 8000 keV; the profiles relative to the glaze show very minor differences for  $K_2O \cdot Al_2O_3$  and  $SiO_2$ . The glaze, which has been analysed from the surface, has evidently a thickness that overcomes  $41.5 \mu m$  (equivalent NIST621 at 7870 keV), otherwise we would have seen larger differences at 8000 keV in MgO and  $SiO_2$ , due to the contribution of the body. Indeed, as it can be observed in Fig. 1, the thickness of the glaze layer oscillates between 110 and  $120 \mu m$ . It is worth recalling that  $\alpha$ -PIXE selects, in the way we used it, a layer corresponding to the range of alpha particles at the given energy and for that layer gives an average composition. Therefore, we can remain within a specific structure (e.g. the glaze) of the analysed sample but we cannot follow a possible concentration variation (e.g. due to diffusion) within the explored layer. The body has been analysed from the side. Therefore, there is no admixture of layers in the  $\alpha$ -PIXE measurements and the presence of elements in the profiles of the body can only be linked to its own composition.

Table 3  
Chemical composition of the colours (in wt.%)

	Black 8 MeV	Black 2.5 MeV	Green 8 MeV	Green 2.5 MeV	Red 8 MeV	Red 2.5 MeV	Yellow 8 MeV	Yellow 2.5 MeV	Yellow 2.5 MeV
Na <sub>2</sub> O	2.45	2.82	1.19	2.45	1.50	2.32	3.38	2.78	2.24
MgO	0.64	0.74	0.26	0.25	0.48	0.48	1.11	0.58	0.88
Al <sub>2</sub> O <sub>3</sub>	2.00	2.08	1.34	1.35	2.14	3.83	15.06	6.12	5.21
SiO <sub>2</sub>	48.19	42.04	18.09	27.38	21.74	24.09	65.36	33.16	29.46
Cl	0.43	0.43	0.10	0.56	0.64	0.51	0.05	0.42	0.49
K <sub>2</sub> O	2.43	2.45	1.20	1.45	1.73	1.96	9.28	3.55	2.63
CaO	1.79	2.20	1.16	1.25	1.33	1.46	1.29	1.48	4.41
MnO	2.66	5.16	0.06	0.63	0.03	0.04	0.01	n.d.	0.03
Fe <sub>2</sub> O <sub>3</sub>	0.33	0.24	0.59	1.10	18.59	24.88	0.40	3.43	6.86
CoO	1.14	1.11	0.03	0.11	n.d.	n.d.	n.d.	n.d.	n.d.
CuO	0.18	0.31	2.63	4.97	0.08	0.25	0.02	0.24	0.17
SnO <sub>2</sub>	5.68	3.94	0.7	0.86	0.2	n.d.	n.d.	n.d.	n.d.
Sb <sub>2</sub> O <sub>5</sub>	n.d.	n.d.	1.01	1.59	1.99	1.62	0.52	1.88	3.45
Au	0.83	1.17	n.d.	n.d.	n.d.	n.d.	n.d.	n.d.	n.d.
PbO	30.35	35.01	45.35	61.4	42.01	39.86	0.26	40.93	41.69

Concentrations of the main components can be reduced to the usual glaze formulation,  $RO \cdot Al_2O_3 \cdot SiO_2$ , where RO are the flux oxides (alkaline, alkaline-earth, PbO or ZnO). The composition determined by 2.5 MeV PIXE or by XRF yields in the formula  $RO \cdot Al_2O_3 \cdot 6SiO_2$  which corresponds to a natural feldspar,  $K(Na)AlSi_3O_8$ . Feldspar, sometimes with small calcium additions, was a usual formula in the European hard porcelains at the end of XVIII century.

Table 3 shows colours composition determined by  $\alpha$ -PIXE. It was previously determined<sup>1</sup> by grazing incidence X-ray diffraction in areas wide enough to perform it, that the abundant colours and shades found in this tiles collection from Aranjuez were made by blending just three pigments: “Naples Yellow,”  $Pb_2Sb_{2-x}Sn_xO_{6.5}$ , “Purple of Cassius”, colloidal gold precipitated by Sn, and “Iron and Manganese Black”,  $Fe_{2-x}Mn_xO_3$ . Oxides were dispersed in a lead rich frit, some times tinted with Cu, Co or other dissolved cations which modified the original pigment colour.

When we analyse the effect of particle range on the concentrations obtained for the pigments, we can observe that the alpha energies (ranges) have been appropriately selected to produce elemental yield only on the painted layers (2500 keV) or partly in the underlying glaze (8000 keV). In Fig. 6 we indeed observe that there is little contamination of the painted layers by the underlying glaze material. All the painted layers maintain, at the two energies, a composition that reflects primarily the composition of the pigments and not that of the underlying parts. The only exception is a yellow brush stroke that is so thin, of the order of the range of alpha particle at 2310 keV, that its contribution to the X-ray spectra at 8000 keV is hidden by that of the feldspar glaze, low in Pb and rich in Al.

As seen in Table 3, the concentrations of PbO in the coloured decoration remains above 30%, even if we subtract the fraction contributed by lead-antimonate, as a characteristic of the  $SiO_2$ -PbO glass frit where pigments were dispersed. The composition of pigments is rather clear. Fig. 6 shows the three main oxides which, beside PbO, are present in the colours. The yellow colour is characterized by a relatively high Sb content (Table 3)

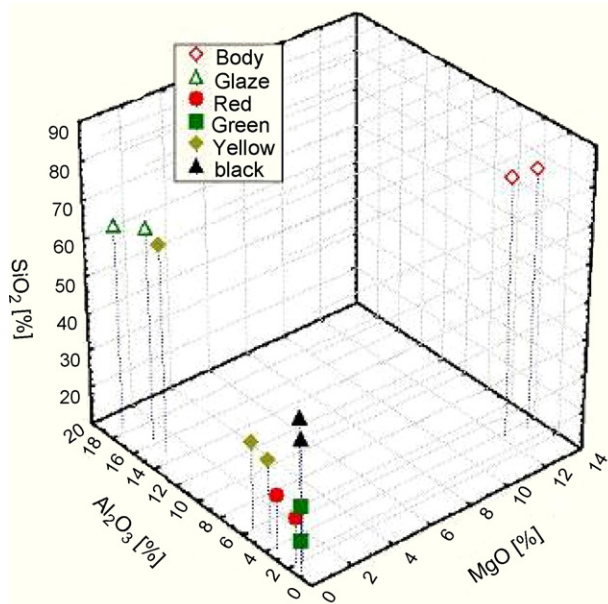


Fig. 6. The concentrations of  $\text{SiO}_2$ ,  $\text{Al}_2\text{O}_3$  and  $\text{MgO}$  clearly separate the body, glaze and painted layers in the examined porcelain.

as corresponds to the Naples yellow, mainly lead-antimonate,  $\text{Pb}_2\text{Sb}_2\text{O}_7$ . In the series analysed before, the  $\text{Pb}_2\text{Sb}_{2-x}\text{Sn}_x\text{O}_{6.5}$  pyrochlore<sup>6</sup> was determined. In the present case, no tin was detected and also the known pyrochlore  $\text{Pb}_2\text{Sb}_{2-x}\text{Fe}_x\text{O}_{6.5}$ <sup>7</sup> is formed. SEM-EDS analyses of the pigment particles, Fig. 7, indicate that iron is included in the small octahedral crystals of pyrochlore but not in the glassy phase. Both recipes for the yellow, by including  $\text{SnO}_2$  or  $\text{Fe}_2\text{O}_3$ , were reported by Sureda in his Notebook as “yellow 1” and “yellow 2”.

Again we observed that the measurement on a yellow stroke at 8000 keV does not match the two other measurements on yellow points since what we observe is mainly the underlying glaze.

The red pigment is essentially based on  $\text{Fe}_2\text{O}_3$ . This pigment, also known as saffron of Mars, was not detected in the previously

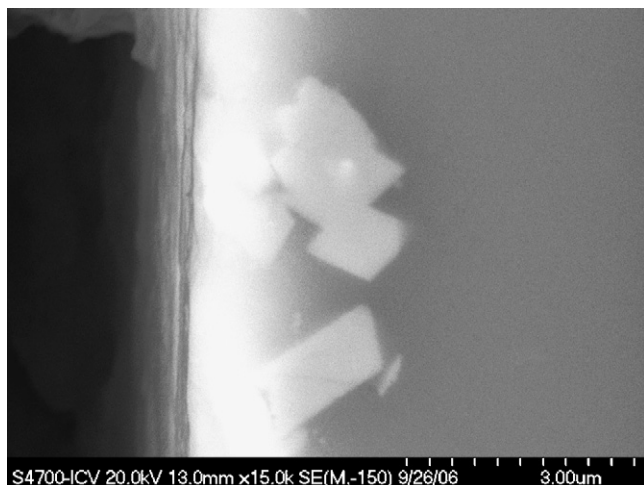


Fig. 7. SEM micrograph of the  $\text{Pb}_2\text{Sb}_{2-x}\text{Fe}_x\text{O}_{6.5}$  crystals in a yellow area of the decoration layer.

identified red tones,<sup>1</sup> but its formulation was also described by Sureda in his Notebook.<sup>8</sup> The small amount of Sb detected must be due to a yellow layer under the red. The green colour is clearly characterized by the presence of Cu, Sb and Sn. After Sureda and the classical ceramic treatises in the XVIII century,<sup>9</sup> green was obtained by modifying the Naples yellow, in this case the Sn doped one, with a Cu and Co rich frit.

In Table 3 we observe the peculiar composition of the black pigment. Fe/Mn concentration ratio is really low if it is compared with the studied black,  $\text{Fe}_{2-x}\text{Mn}_x\text{O}_3$  bixbyite structure, pigment. In this case, the basic manganese black is modified with Cu and Co oxides. Both black formulas are, respectively, described as “other black, as prepared in Sèvres” and “vivid black, as prepared in Madrid” in the Sureda’s Notebook. The presence of Au and  $\text{SnO}_2$  clearly indicates an over painted stroke of “Purple of Cassius”.

The pigment, or its constituent oxides, was mixed and fused in a lead rich flux and, after quenched and ground, painted on the glaze surface and then fired. Special care was taken to find the correct pigment/frit ratio for every colour that could be fired at the same temperature to produce a continuous and thin layer without change in the pigments chemistry.<sup>10</sup>

#### 4. Conclusions

The  $\alpha$ -PIXE technique has made possible the non-destructive characterization of the three main parts of a porcelain sample, representative of the polychrome Sureda production in Buen Retiro. By an appropriate choice of the beam energy it has been possible to confirm, in the simplest way, the layered structure of the sample, as a complement to the necessarily destructive SEM observations. The  $\alpha$ -PIXE has also disentangled the compositional structure of the layers, in particular the painted brush strokes, being capable of determining the pigment composition with high spatial accuracy in all three dimensions (including along the layer thickness) free of interferences from underlying layers, which was not possible with other analytical techniques. The use of the in air micro-beam at the CMAM of Madrid has made the measurements totally non-destructive.

#### Acknowledgements

The authors wish to thank J.G. Zubiri, O. Enguita, A. Rodríguez and J. Narros, for the technical support and operation of the accelerator. One of us (A.Z.) is particularly indebted to the Centro de Micro Analysis de Materiales of the Universidad Autonoma de Madrid for financial support and to the staff of that centre for friendly and restless collaboration. Finally, authors would like to acknowledge to J.L. Valverde and to *Patrimonio Nacional* the opportunity of studying one of the stored tiles from *La Casita del Labrador*.

#### References

- Pascual, C., Recio, P., Valle, F. J., Criado, E., De Aza, A. H., Martínez, R. et al., The last period of “Buen Retiro” porcelain factory. *Heritage, Weathering and Conservation*. Taylor & Francis, London, 2006, pp. 135–141.

2. De Aza, A. H., De La Torre, A. G., Aranda, M. A. G., Valle, F. J. and De Aza, S., Rietveld quantitative analysis of Buen Retiro Porcelains. *J. Am. Ceram. Soc.*, 2004, **87**(3), 449–454.
3. Enguita, O., Fernández-Jiménez, M. T., García, G., Climent-Font, A., Calderón, T. and Grime, G. W., The new external microbeam facility at the 5 MV Tandatron accelerator laboratory in Madrid: beam characterisation and first results. *Nucl. Instrum. Methods*, 2004, **B219–220**, 384–388.
4. Climent-Font, A., Agullo-Lopez, F., Enguita, O., Espeso-Gil, O., Garcia-Lopez, G. and Pascual-Izarra, C., In *Proceeding CAARI 2000 AIP Conference Proceeding, Vol 576*, 2001, p. 643.
5. Maxwell, J. A., Teesdale, W. J. and Campbell, J. L., The Guelph PIXE software package II. *Nucl. Instrum. Methods B*, 1995, **95**, 407–413.
6. Cascales, C., Alonso, J. A. and Rasines, L., The new pyrochlores  $\text{Pb}_2(\text{MSb})\text{O}_{6.5}$  (M = Ti, Zr, Sn, Hf). *J. Mater. Sci. Lett.*, 1986, **5**, 675–677.
7. Cascales, C., Rasines, I., García Casado, P. and Vega, J., The new pyrochlores  $\text{Pb}_2(\text{M}_{0.5}\text{Sb}_{1.5})\text{O}_{6.5}$  (M = Al, Sc, Cr, Fe, Ga, Rh). *Mater. Res. Bull.*, 1985, **20**, 1359–1365.
8. Sierra Alvarez, J. and Tuda Rodríguez, I., *Sureda Miserol, Bartolomé, Cuaderno de notas sobre cerámica*. Museo Municipal, Madrid, 2000, pp. 1802–1826.
9. Didier D'Arclais de Montamy, *Traité des couleurs pour la peinture en émail et pour la porcelaine*. Paris, 1765.
10. Lowengard, S., Chemistry in colour: ceramics and glass in 18th-century Britain. *Endeavour*, 2002, **26**, 102–106.